Cable Design and Development for the High Temperature Superconductor Cable Test Facility Magnet

Ian Pong, *Senior Member, IEEE,* Aurelio Hafalia, Hugh Higley, Elizabeth Lee, Andy Lin, Michael Naus, Carlos Perez, Soren Prestemon, *Senior Member, IEEE*, GianLuca Sabbi, Simon C. Hopkins, Amalia Ballarino, Luca Bottura

***Abstract*— A large bore "High Temperature Superconductor Cable Test Facility Magnet" for testing advanced cables and inserts in high transverse field is in its design phase. This magnet will be the core component of a facility for developing conductors and accelerator magnets operating above 15 T, an enabling technology for next-generation fusion devices using magnetic confinement of plasma and for future energy frontier colliders. The procurement of Nb_3Sn conductor, fabrication of cables, winding of coils, and assembly of the dipole magnet will be done at Lawrence Berkeley National Laboratory (LBNL) and the test pit and cryostat will be constructed at Fermi National Accelerator Laboratory (FNAL). This paper will present the conductor element of the LBNL project, specifically cable design parameters (based on the Bruker OST RRP® Nb_3Sn superconducting wire) and the development phase cable fabrication experience. Challenges of the cable fabrication will be discussed. The wire and cable planned for this magnet are similar to those under study for the Future Circular Collider and other large facility magnets. The successful fabrication of the development cable has positive implications for these other projects.**

***Index Terms*—Fusion, High Energy Physics, FCC, Nb_3Sn, accelerator magnets**

I. Introduction

THE "High Temperature Superconductor Cable Test Facility", to be operated at FNAL, will be used to test high temperature superconductor cables with high current (20 kA up to possibly 100 kA) in a variable temperature insert (up to 50 K or even ~100 K) in a large, rectangular, bore (~100 × 150 mm^2) magnet at high background field (~15 T at 4.2 K, or ~16 T at 1.9 K).

The establishment of this facility comprises two projects. The cryostat procurement, test pit preparation, installation, etc., are a Fermi National Accelerator Laboratory (FNAL) project [1]. The magnet assembly, coil fabrication, and conductor (wire procurement and cable fabrication) are an LBNL project known internally as the "Test Facility Dipole" project, or TFD. The paper is about the conductor element of the TFD only.

The TFD magnet (Figure 1) will, according to the conceptual design [1], [2] weigh not much more than ~20 t due to building facilities limitation (maximum 25 t), and be <1.3 m in diameter as limited by the planned cryostat dimensions. The dipole magnet will contain two "coil modules". Each module (not including the axial loading rods) will be ~ 2.5 m-3.0 m long, weigh ~2,000 kg, and have two 2-layer coils ("flared end race track", a.k.a. block coil). Each 2-layer coil will be wound with one continuous length of Nb_3Sn Rutherford cable. The maximum length of the cable is limited by the LBNL cabling machine load capacity (~200 kg of wire).

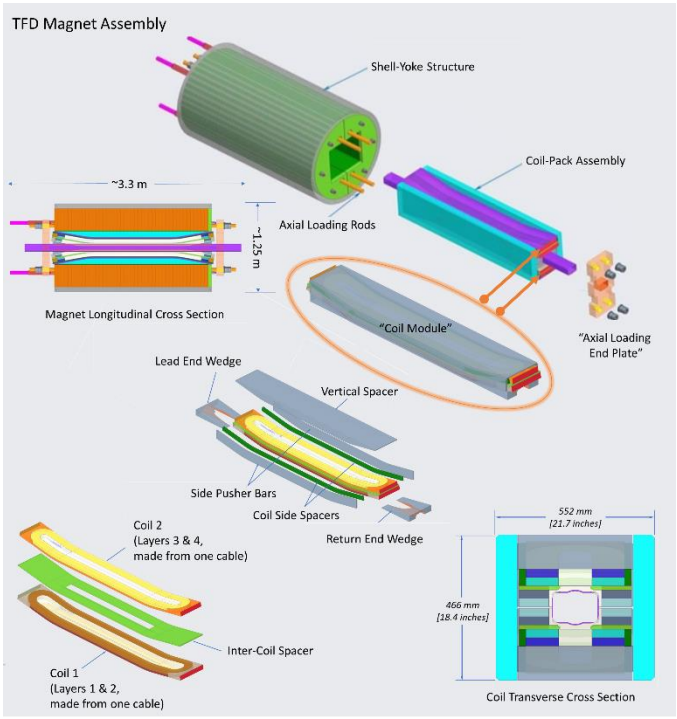

Figure 1: Test Facility Dipole (TFD) magnet assembly schematic broken down to show the shell-yoke structure, the coil-pack assembly, the coil module, and individual 2-layer coils. Also shown are the magnet longitudinal cross section and coil transverse cross section with dimensions.

Manuscript receipt and acceptance dates will be inserted here. The work performed at Lawrence Berkeley National Laboratory was supported by the Office of Science, U. S. Department of Energy, under contract No. DE-AC02-05CH11231 *(Corresponding author: Ian Pong.)*

Ian Pong, Soren Prestemon, and GianLuca Sabbi are with the Accelerator Technology & Applied Physics (ATAP) Division, Lawrence Berkeley National Laboratory (LBNL), 1 Cyclotron Road, Berkeley, CA 94720-8201, U.S.A. (e-mail: ipong@lbl.gov, soprestemon@lbl.gov, glsabbi@lbl.gov).

Aurelio Hafalia, Hugh Higley, Elizabeth Lee, Andy Lin, Michael Naus, and Carlos Perez are with the Engineering Division, Lawrence Berkeley National Laboratory (LBNL), 1 Cyclotron Road, Berkeley, CA 94720-8201, U.S.A. (e-mail: rrhafalia@lbl.gov, hchigley@lbl.gov, emlee@lbl.gov, andylin@lbl.gov, naus@lbl.gov, caperez@lbl.gov)

Simon Hopkins, Amalia Ballarino, and Luca Bottura are with the Magnets, Superconductors and Cryostat Group at the European Organization for Nuclear Research (CERN), CH-1211 Geneva 23, Switzerland (e-mail: simon.hopkins@cern.ch, amalia.ballarino@cern.ch, luca.bottura@cern.ch).

Color versions of one or more of the figures in this paper are available online at http://ieeexplore.ieee.org.

Digital Object Identifier will be inserted here upon acceptance.

According to the project plan, 8 cable runs are anticipated in three phases, all to be done at LBNL:

- One "Development" effort making short units (a few pieces ~10 m each) using different values around the nominal target of some selected parameter(s) for winding tests. Wire were procured by LBNL and CERN in 2019.
- One "Prototype" cable (~400-500 m, expected to be made before the end of 2021) for the "Prototype" coil (a full-size coil built for feedback on design and fabrication), made from wire to be procured under a "TFD Wire Specification for a Prototype Cable" [3] before the Conductor Design Review (CDR) which is expected to take place in spring 2021.
- Four "Production" cables for the magnet and two "Spare" cables for the spare coils, expected to be made in 2022-2023. Wire used for the production and spare cables will be procured under "TFD Wire Specification for the TFD coils", a document to be approved by the project following CDR.

This paper will focus on the cabling design, planning efforts, and our first phase, the so-called development cable fabrication experience.

II. Wire

Two wire spools were acquired:

- Wire ID WO11S00545A02U acquired by LBNL. Its nominal length is 3130 m. It is an RRP® wire manufactured by Bruker OST with a 108/127 restack design according to the US-HL-LHC Accelerator Upgrade Project (AUP) specification [4], [5], but at 1.1 mm diameter. It uses subelements with a "reduced Sn" Nb:Sn ratio of 3.6:1 and has a nominal wire Cu:non-Cu ratio of 1.2.
- Wire ID CO11S20235A04U acquired by CERN. Its nominal length as sent to LBNL is 3136 m. It is an RRP® wire manufactured by Bruker OST with a 162/169 restack design according to a specification for high field magnet development activities [6]. The wire diameter is 1.1 mm. It uses subelements with a "standard Sn" Nb:Sn ratio of 3.4:1 and has a nominal wire Cu:non-Cu ratio of 0.9.

Two cable maps were planned. Their identification (as will be used in the rest of this paper) are:

- Cable W10OL1301 using WO11S00545A02U.
- Cable W12OL1302 using CO11S20235A04U.

III. Cable Design

Some of the cable baseline design considerations are driven by the magnet and coil designs [7]-[10], or by cabling factors, whereas others require balancing a combination of both.

The target range for the cable width is mainly determined by the magnet bore size and the number of coil layers. Given the wire diameter options (1.1 mm and 1.0 mm were both considered during conceptual design, but 1.1 mm is preferred), the number of strands is quickly settled at 44 for 1.1 mm or 48 for 1.0 mm strands to achieve a 26.0 ± 0.3 mm wide cable.

TABLE I
Design Targets for the Development Cable

Parameter	Lower Limit	Target Value	Upper Limit
No. of strands	43	44	44
Cable width	25.7 mm	26.0 mm	26.3 mm
Cable thickness[a]	1.87 mm	1.92 mm	1.97 mm
Cable pitch	125 mm	155 mm	185 mm
Residual twist (24 kg)[b]	-	ALARA[c]	<150°/m

[a] Cable cross section parameters of unreacted cables measured using the Cable Measurement Machine (CMM) at a set pressure of 14 MPa on the broad face
[b] Residual twist is measured over 1 m under 24 kg by noting the twist in degrees.
[c] ALARA: As low as reasonably achievable.

Due to mechanical stability and manufacturability considerations, the cable target twist pitch (also known as the transposition pitch or cable lay pitch) angle range is set between 15° and 23°, giving a pitch length of approximately 155 mm ± 30 mm. The compactness at the cable edge can be adjusted by the cable pitch length or by changing the width.

The cable thickness target range is chosen based on the general rule of 10-15% thickness reduction, which at 1.1 mm strand diameter and without a cable core is 1.92 ± 0.05 mm. This parameter is considered to be one that requires compromising in the final design decision, because higher compaction typically gives better coil winding mechanical stability but worse degradation in the cable residual resistance ratio (RRR), typically assessed via extracted strands. It is therefore a priority parameter whose window of acceptability is to be explored during this development phase.

A requirement of the block coil design is a flat rectangular cable with no keystone angle and minimum residual twist. From LBNL's cabling experience, low residual twist can be achieved effectively by a low temperature pre-cabling annealing. An alternative would be to make the cable using a two-pass procedure with intermediate annealing. We chose the single-pass procedure with pre-cabling annealing because the risk, labour cost, and number of hardware parts involved are lower. The pre-cabling annealing recipe will be described below in section IV.

A requirement associated to magnet stability is a reasonably high conductor RRR---an often accepted value being >100 [11]. Since RRR degradation in Nb_3Sn cables is caused by sheared subelements releasing Sn into the stabilizing Cu matrix, transverse cross section metallography assessment of the number of subelements damaged is a quick and convenient way to estimate the RRR degradation without the need to perform heat treatment and cryogenic measurements, which usually take at the very least two weeks. Another assessment, which is even more immediate and non-destructive, though a little less precise, is facet size image analysis. Both techniques are known to have a good association to RRR values [12]. Although their correlation in the TFD cables has yet to be established, an aim of the development effort is to compare the initial cabling results to datasets with much better statistics such as AUP [12].

The key target parameters are summarized in Table I.

IV. Preparation

To prepare for the fabrication of the large diameter wire, 44-strand cable with an estimated ~300 kg tension (due to ~7 kg of tension per strand applied through spool and capstan brakes and due to friction), we upgraded our powered Turkshead motors and circuitry from a pair of ~32 N·m (supplier specification: 280 in-lbs.) DC gear motors made by Bodine Electric Company driven *in series* by a single power supply [13] to a pair of ~40 N·m (supplier specification 350 in-lbs.) DC gear motors rated 90 V at 2.2 A and 21 rpm by the same brand, driven *separately* by two TDK Lambda Z+ series power supplies.

Upon receiving the wires, we took short samples and performed pre-annealing (i.e. as-received) QC—including metallography, spring back (to determine the amount of spring back of a wire after 10 complete turns on a 10 mm diameter shaft under a 2 kg load [14]), and self-bend (to determine if the sample can survive without cracking or observable surface defects when bent on itself [15])—, a couple of test annealing experiments, and post-annealing QC (same QC as pre-annealing) to determine the pre-cabling annealing heat treatment, which was eventually set at 170°C for 16 h.

The pre-cabling annealing of both WO11S00545A02U and CO11S20235A04U was done simultaneously in a single retort under flowing argon according to our Wire Annealing Procedure [16]. Due to the thermal mass involved, the hub end of the spools and the free end (i.e. top) of the spools saw some observable temperature difference. The dwell temperature start was defined as when a thermocouple (TC) first crossed 165°C (target temperature minus 5°C), and the finish as when the last TC crossed below 165°C. Based on this, the hub and top of the spools experienced 17 h and 19.4 h of annealing above 165°C, respectively. See Figure 2.

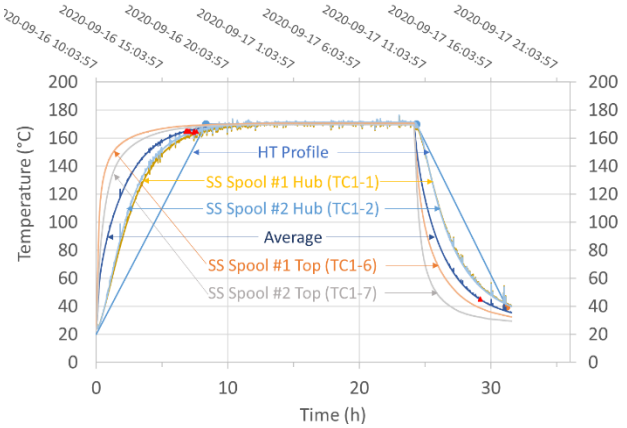

Figure 2 Pre-cabling annealing profile and thermocouple records. CO11S20235A04U was on stainless steel (SS) spool #1 whereas WO11S00545A02U was on stainless steel (SS) spool #2.

The inspected wire diameter during respooling grew by approximately 1 µm after annealing for both wire spools, with a slightly increased standard deviation compared to before annealing. The annealing caused a modest increase in spring back degree from about 450° to 510° and in spring back diameter from 11.1 mm to 11.4 mm. All as-received and annealed samples passed the self-bend test.

V. Cabling Results and Experience

In total, nearly 60 m each of W10OL1301 and W12OL1302 were successfully fabricated in several sections for in-process (i.e. with immediate feedback while cabling paused) and post-process (i.e. after the conclusion of the development phase of cabling efforts) coil test winding. As cable thickness is our priority parameter whose window of acceptability is to be explored, these sections were made with different thicknesses.

A very low residual twist of 15° to 25° and in the favourable direction (i.e. the residual twist tightens under load) was achieved from the beginning and in both W10OL1301 and W12OL1302. This confirms that the design choice of applying pre-cabling annealing can achieve residual twist values similar to the two-pass cables with intermediate annealing used by past LBNL race-track coil or block coil magnet projects.

In terms of the cable transverse cross section parameters, the cable was very flat (keystone angle measured by CMM was 0.05° or less) and the cabling team managed to control the width and thickness from the start so close to target that a number of exploratory units were made to test the windability window and to attempt facet size reduction, including thickness variation, dropping a strand (43-strand cable), and running with the horizontal rollers opened. See Figure 3. Although crossover-free cables could be made with the horizontal rollers opened, the hardware was not optimized for the increased width. It is not a standard cabling procedure but is acceptable at this development phase and was used to explore the possible width window without investing into dedicated hardware.

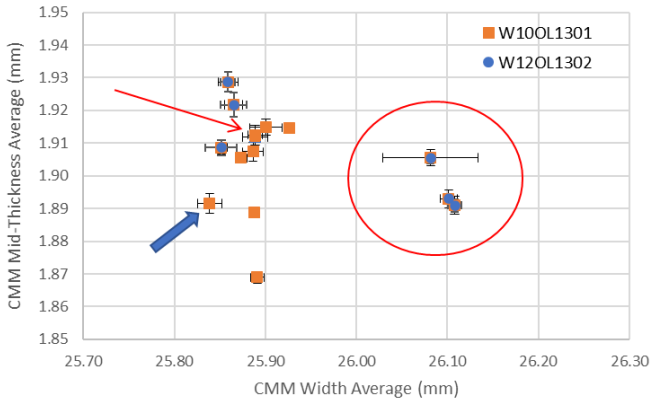

Figure 3 CMM data: mid-thickness plotted against width. The thin arrow points at the very first startup sample made, showing the level of control achieved. Subsequently a range of thickness was explored to test the windability window. A few pieces (in red circle) were also made with the horizontal rollers opened by ~0.25 mm to achieve an increased width. The thick arrow points at the 43-strand sample.

The facet size of each section is analysed using a custom script written in ImageJ/FIJI on images acquired by a Keyence Vision system. An example image is shown in Figure 4. The cable is too wide for our present setup to image the entire broad face and both edges. For short startup pieces, we could re-run the cable pieces upside-down a second time to image the other edges, but not for longer pieces without respooling. The facet length varies among the samples fabricated, depending on the

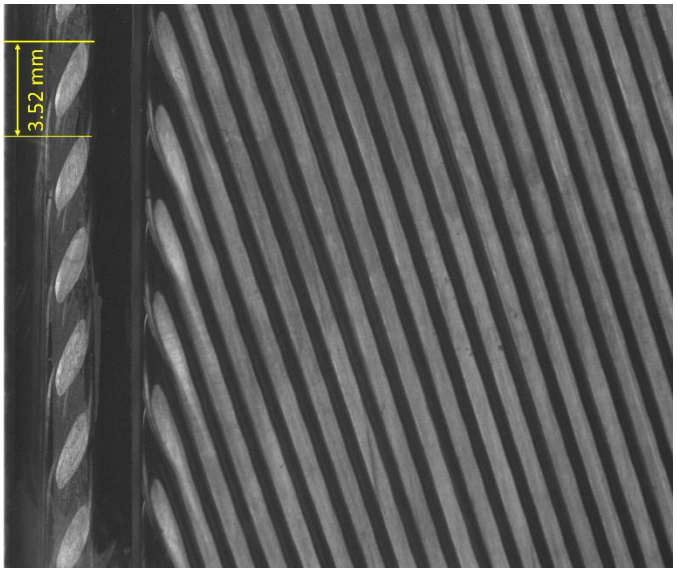

Figure 4 Example of a Keyence Vision system acquired image. The cable twist pitch is 155 m. With 44 strands, each facet period is approximately 3.52 mm. This image is of the "positive-x" edge from sample W10OL13011A00A. The facet sizes vary in the samples made using different parameters. A single image may not be statistically representative of the average facet in longer cables produced in planetary steady state.

amount of compaction (thickness and width), from obviously not overlapping such as in Figure 4 to just overlapping. Since many of the sample lengths were not produced in a planetary steady state, the facet stability statistics will be studied during the Prototype cabling phase. (Each of the strands is paid out from a spool mounted on a fork with a rotation about the fork's axis and a revolution around the turning base plate ("bay") – the spools are thus in a planetary orbital motion. The distance for the twist on the strands to stabilize is typically a few times the path length between the payout and the Turkshead.)

Transverse cross section micrographs on W10OL1301 samples reveal that the extent of sheared damage of subelements in the triplet position is not significant (Figure 5)—comparable to the AUP (MQXFA) cable samples, which are made from the same wire design at a smaller (0.85 mm) diameter. Sheared subelements are typically along 45° lines, crossing the wire like an "X". Our rule-of-thumb criterion is not more than 15% of sheared subelements, corresponding to 16 sheared subelements in the 108/127 wire design (i.e. shearing each subelement across the four rings at the four diagonal positions) or 24 sheared subelements in the 162/169 wire design (which has six rings of subelements). We counted the number of sheared subelement in 18 wires at six triplets of samples from W10OL1301: 12 of them had no sheared subelements, and the worst of the remaining six had seven out of 108 subelements sheared. Scoring per triplet gives an average of 1.5% sheared subelements with a standard deviation of 1.2%. This compares favourably to AUP cables which have an average score of 4% and a standard deviation of 1.9%.

Since AUP cables' extracted strand RRR agrees well with Bruker OST's 15% rolled strand QC [12] and the TFD will likewise use Bruker OST's RRP® strand with the same subelement

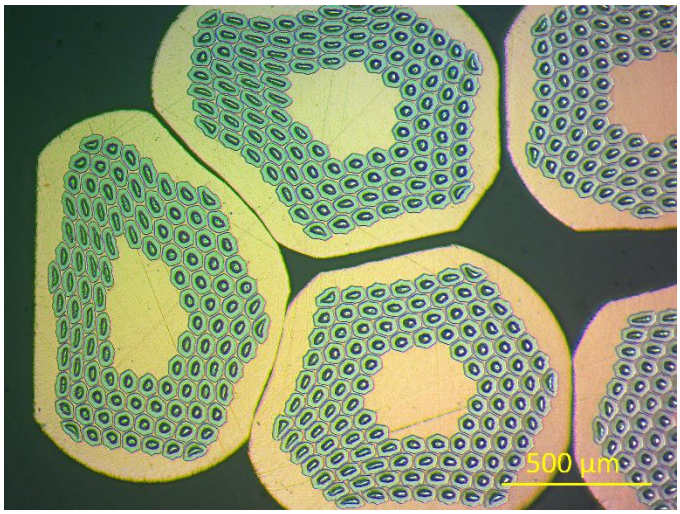

Figure 5 An example transverse cross section micrograph showing little sheared damage to the subelements at the triplet position (i.e. at the cable edge mid-length of the facet). This is the "positive-x" edge from sample W10OL13014A00A.

design, it is expected that the TFD cable's extracted strand RRR can be likewise predicted. The early indication is that the facet size and number of sheared subelements behave similarly to AUP, although further evaluation will be needed to improve the statistics.

Most of the samples were made at < 1 m per minute. However, in order to test the Turkshead motor and power supply capability, during the fabrication of two of the longer pieces, we accelerated up to about 3 m per minute. This did not overload the upgraded Turkshead motor system.

In fact, our cabling experience shows that the most straining part of the fabrication (requiring the highest torque to be delivered by the Turkshead) is not during acceleration or top speed fabrication but during startup, when there are crossover defects to be passed through the Turkshead aperture.

During W12OL1302 startup, our operator heard an unusual sound near the Turkshead. At the time, the Turkshead setting was at target thickness and procedural distance from the mandrel pinch point. After the cable run was completed and the rollers taken out, we found the keyway slot of both vertical rollers were cracked (Figure 6). After consultation with an expert machinist, it is believed that an improved design with a radiused keyway machined before hardening heat treatment could prevent stress concentration effectively. From the operation procedure point of view, it may also help limit the required torque and may give better control to start at a fraction of a mm oversize in thickness to allow crossovers to pass before closing on to target thickness.

Another challenge caused by the high total strand tension and high torque required is that the equal and opposite reaction force to that delivered by the motors pulls the lathe bridge on which the Turkshead is mounted upstream towards the rotating bay. While slippage during cable fabrication can be prevented by locking down the bridge, it makes startup alignment adjustment ("pinch point checking") difficult and more prone to damaging hardware components.

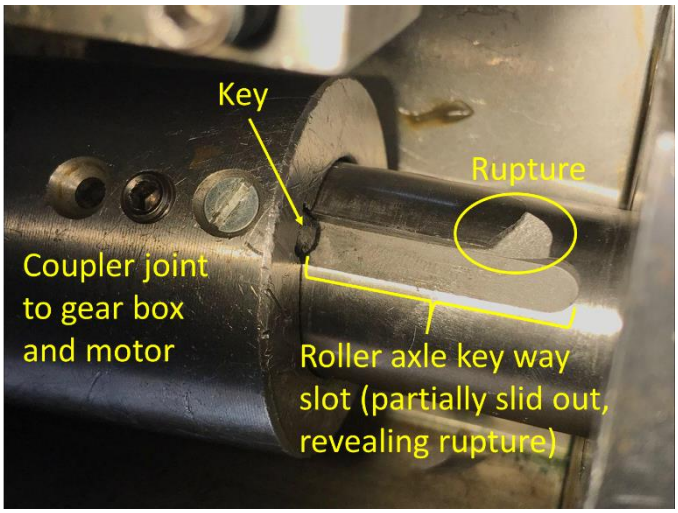

Figure 6 Photograph showing one of the ruptured roller axle key way slots discovered after cabling during Turkshead disassembly. The joint is partially disassembled with the coupler joint exposed to reveal the rupture next to the roller axle key way slot.

VI. Conclusion

The development cable fabrication showed promising results and provided assuring experience, which bode well for the project. Pre-cabling annealing proved to be an appropriate choice to minimize residual twist and the Turkshead motor upgrade was crucial to deliver the necessary power to fabricate cable of this size. The high torque and high tension gave challenges and may require roller design modification. From the project point of view, acquiring a spare mandrel and set of rollers could mitigate a schedule risk due to hardware components suffering unexpected damage. Extrapolating from AUP experience, the facet size and transverse cross section metallography suggest cable (extracted strand) RRR may be plausibly predictable from rolled wire QC during wire acceptance. This will be validated in future experiments and the next phase of the project.

Acknowledgment

The authors are grateful to LBNL QEWs Jordan Taylor and Patricius "Rick" Bloemhard for assisting the Turkshead upgrade, and to LBNL technician supervisor Tom Lipton for roller improvement discussions.

References

[1] G. V. Velev, C. Sylvester, D. Arbelaez, V. Kashikhin, S. Koshelev, V. Marinozzi, *et al.*, "Design and Construction of a High Field Cable Test Facility at Fermilab", *IEEE Transactions on Applied Superconductivity*, vol. 31, no. 5, Aug. 2021. Article No. TBC. Presented at ASC 2020 Wk2LPo3F-06 and under review. Poster: https://asc2020.ipostersessions.com/Default.aspx?s=AD-09-18-61-5A-BE-89-29-1D-80-72-3F-B7-F7-74-58; https://doi.org/10.1109/TASC.2021.3068847

[2] Test Facility Dipole Conceptual Design Review https://conferences.lbl.gov/event/359/

[3] I. Pong, "LBNL Test Facility Dipole Project Wire Specification for a Prototype Cable", LBNL Document, DF-1000-0602 https://pdmlink.lbl.gov/Windchill/app/#ptc1/tcomp/infoPage?oid=OR%3Awt.doc.WTDocument%3A996735272&u8=1

[4] L. D. Cooley, A. K. Ghosh, D. R. Dietderich, and I. Pong. "Conductor specification and validation for high-luminosity LHC quadrupole magnets." *IEEE Transactions on Applied Superconductivity*, vol. 27, no. 4, June 2017. Article No. 6000505. https://doi.org/10.1109/TASC.2017.2648738

[5] L. D. Cooley, " US-HiLumi Document 40-v10 Specification for Quadrupole Magnet Conductor" [Online]. Available: https://us-hilumi-docdb.fnal.gov/cgi-bin/private/ShowDocument?docid=40

[6] "Technical Specification - Supply of Nb_3Sn Wires for the FCC Study at CERN", CERN EDMS No.: 1835808, IT-4363/TE/FCC Document Reference FCC-ACC-PR-0001 January 30, 2019. https://edms.cern.ch/document/1835808

[7] P. Bruzzone, L. Bottura, F. Cau, G. de Rijk, P. Ferracin, J. Minervini *et al.*, "Conceptual design of a large aperture dipole for testing of cables and insert coils at high field," *IEEE Transactions on Applied Superconductivity*, vol. 28, no. 3, Apr. 2018. Article No. 4005505. https://doi.org/10.1109/TASC.2017.2785828 .

[8] X. Sarasola, P. Bruzzone, L. Bottura, P. Ferracin, D. M. Araujo, G. de Rijk *et al.*, "Magnetic and mechanical design of a 15 T large Aperture dipole magnet for cable testing," *IEEE Transactions on Applied Superconductivity*, vol. 29, no. 5, Aug. 2019, Article No. 4001405. https://doi.org/10.1109/TASC.2019.2896954.

[9] G. Vallone, D. Arbelaez, D. M. Araujo, A. Ballarino, P. Ferracin, A. Hafalia *et al.*, "Magnetic and Mechanical Analysis of a Large Aperture 15 T Cable Test Facility Dipole Magnet", *IEEE Transactions on Applied Superconductivity*, vol. 31, no. 5, Aug. 2021. Article No. 9500406. https://doi.org/10.1109/TASC.2021.3065882

[10] D. M. Araujo *et al.*, "Magnetic and mechanical 3-D modelling of a 15 T large aperture dipole magnet", *IEEE Transactions on Applied Superconductivity*, vol. 30, no. 4, Jun. 2020. Article No. 4000705. https://doi.org/10.1109/TASC.2020.2969639.

[11] B. Bordini, L. Bottura, L. Oberli, L. Rossi, and E. Takala. "Impact of the Residual Resistivity Ratio on the Stability of Nb_3Sn Magnets", *IEEE transactions on applied superconductivity*, vol. 22, no. 3, Jun. 2011. Article No. 4705804. https://doi.org/10.1109/TASC.2011.2180693

[12] I. Pong, M. Naus, E. M. Lee, "302.2.03 Report on Cable P43OL1139". [Online]. Available: https://us-hilumi-docdb.fnal.gov/cgi-bin/private/ShowDocument?docid=3337

[13] E. M. Lee, "77A Motor Wiring Analysis Spring 2020", LBNL Engineering Technical Note, SU-1012-3217. https://pdmlink.lbl.gov/Windchill/servlet/AttachmentsDownloadDirectionServlet?oid=OR:wt.doc.WTDocument:836179382&oid=OR:wt.content.ApplicationData:836179727&role=PRIMARY

[14] I. Pong, "HFTFD Determination of Springback Properties", LBNL Procedure, SU-2220 DF-1000-0725 Rev. A https://pdmlink.lbl.gov/Windchill/servlet/AttachmentsDownloadDirectionServlet?oid=OR:wt.doc.WTDocument:1062728605&oid=OR:wt.content.ApplicationData:1062728640&role=PRIMARY

[15] I. Pong, "Self-Bend Pass/No Pass Test", LBNL Procedure, SU-2230 DF-1000-0726 Rev. A. https://pdmlink.lbl.gov/Windchill/servlet/AttachmentsDownloadDirectionServlet?oid=OR:wt.doc.WTDocument:1062735781&oid=OR:wt.content.ApplicationData:1062735907&role=PRIMARY

[16] E. M. Lee, M. Naus, I. Pong, "TFD Wire Pre-Cabling Annealing Procedure", LBNL Procedure, SU-1012-8040 https://pdmlink.lbl.gov/Windchill/servlet/AttachmentsDownloadDirectionServlet?oid=OR:wt.doc.WTDocument:978317944&oid=OR:wt.content.ApplicationData:978324135&role=PRIMARY